Study of the thermal stability of the natural zeolite heulandite

F. PECHAR and D. RYKL

Institute of Geology and Geotechnics, Czechoslovak Academy of Sciences, CS-182 09 Prague

Received 10 October 1983

Accepted for publication 31 July 1984

On the basis of the course of the DTA and TGA curves the natural zeolite heulandite (Poonah locality, India) was subjected to the isothermal decomposition at the various temperatures (θ/°C: 20, 200, 280, 470, 510, 620, 660, 760, 820, and 1000). The decomposition products were studied by means of the X-ray powder methods and by the infrared absorption spectroscopy. It was found that the heulandite structure is stable up to the temperature of 280 °C. At the temperature exceeding 280 °C the transformation into the modification of heulandite B occurs. From the temperature of 470 °C upwards the amorphous phase begins to be formed, from which at the temperature exceeding 500 °C a mixture of minerals wairakite + α-SiO_2 and/or anorthite + SiO_2 starts to appear. In the course of dehydration starting from 200 °C, in the cavities of heulandite simultaneously proceeds the heterolytic reaction, at which the free proton is formed, which immediately attacks the bridge oxygens in the bridge Al—$\overset{(-)}{O}$—Si under the formation of hydroxyl groups. These groups partly remain in the complicated complex up to the high temperatures.

На основе хода кривых ДТА и ТГА, природный цеолит гейландит (месторождение Поонах—Индия) подвергался изотермическому разложению при разных температурах (θ/°C: 20, 200, 280, 470, 510, 620, 660, 760, 820, 1000). Продукты разложения изучались методами рентгеновских порошкограмм и инфракрасной абсорбционной спектроскопии. Было определено, что структура гейландита стабильна до температуры 280 °C. Выше этой температуры наступает переход в модификацию гейландит B. При температуре 470 °C начинает образовываться аморфная фаза, из которой, в свою очередь, образуется при температуре выше 500 °C смесь вайракит + α-SiO_2 или анортит + α-SiO_2. В течение дегидратации, начиная от 200 °C протекает в пустотах гейландита одновременно гетеролитическая реакция, в результате которой возникает свободный протон, сразу же атакующий мостиковый кислород связи Al—$\ddot{O}$—Si, что вызывает образование гидроксильных групп. Эти группы частично сохраняются в сложном комплексе до высоких температур.

A great attention was paid to the study of thermal stability of zeolites both in the dynamic [1—8] and in the isothermal regime [8] in connection with their application in the technical practice [9, 10]. All studies were aimed especially at the synthetic analogues of zeolites and of the natural ones at those which can be applied in the chemical industry — chabazite, faujasite, mordenite, and klinoptilolite. There exist some summarizing papers on heulandite [6, 7, 11—13] describing especially the evaluation of DTA, TGA curves and X-ray patterns under the increasing temperature. With regard to the fact that these measurements were carried out under the dynamic equilibrium regime, in which many effects cannot be well distinguished, it was necessary to complete them by the isothermal measurement. Simultaneously there were followed the decomposition products by means of the X-ray diffraction analysis and by the infrared absorption spectroscopy. The X-ray measurements are not able to record the property changes of the zeolite water in the course of dehydration. Heulandite, conformably to *Breck* [9], belongs into the 7th structural zeolite group (monoclinical, space group Cm). The basic skeleton of zeolites of this group is created by the secondary building units 4-4-1. The diameter of the free structural cavities of this mineral is as follows:

1. 0.4×0.5 nm in 8-group circles, which are perpendicular to the crystal *a* axis;
2. 0.4×0.7 nm in 10-group circles, perpendicular to the crystal *c* axis;
3. 0.4×0.47 nm in 8-group circles, perpendicular to the crystal *c* axis.

In these cavities there are the fully hydrated cations Ca^{2+} in aquacomplex [9]. Each ion Ca^{2+} is coordinated with five water molecules and three skeleton oxygens, belonging into the bridge Al—$\overset{(-)}{O}$—Si [9].

According to the relation $n(Si) : n(Al) = 3 : 2.5$ it can be deduced that heulandite belongs among the zeolites with a relatively high aluminium content in the structure, the consequence of which is a lower temperature stability of this mineral (destabilizing effect) [9]. In accordance with the anisotropic mobile water molecules we can say that the dehydration will be realized in a large thermal interval under the formation of a transitory mineral metaphase [9].

Experimental and results

The crystallic heulandite samples (Poonah locality, India) were subjected to the chemical quantitative analysis (the analyses were carried out by the experts of the analytical laboratory of the Institute of Geology and Geotechnics of the Czechoslovak Academy of Sciences under the control of Ing. V. Chalupský), the results of which are indicated in Table 1. From this analysis the following crystallochemical formula was calculated

$$(Na_{1.14}K_{0.06}Ca_{3.84})[(Al_{8.51}Fe_{0.06}Si_{27.22})O_{72}] \quad 28.64H_2O$$

which is in principle conformable with the theoretical formula $Ca_4[(Al_8Si_{28})O_{72}] \quad 24H_2O$. It differs only as for the sodium and water content.

Table 1

Chemical composition of heulandite

Oxide	*w* /%	
	Theoretical	Poonah, India
SiO_2	61.26	57.43
Al_2O_3	14.85	15.24
Na_2O	—	1.24
K_2O	—	0.10
CaO	8.17	7.58
MgO	—	0.09
MnO	—	0.0002
Σ Fe_2O_3	—	0.16
Σ H_2O	15.72	18.10
Σ	100.00	99.94
$m(Si)/m(Al)$	3.642	3.331
$m(Si)/(m(Si)+m(Al))$	0.785	0.769

The TGA and DTA curves (Figs. 1 and 2) were scanned on the device NETSCH Co. at the temperature increase velocity in the standard of 10 °C/min and at the portion of heulandite sample of 50 mg. The evaluation results of TGA and DTA curves are stated in Table 2. The course of these curves is in principle conformable with the curves given in the paper by *Peng* [8]. The isothermal decomposition at the various temperatures (θ/°C: 20, 200, 280, 470, 510, 620, 660, 760, 820, and 1000; the decomposition temperatures were

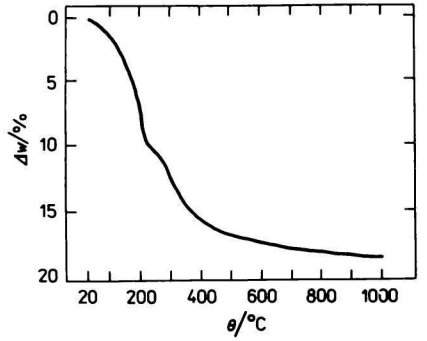

Fig. 1. TGA curve of heulandite.

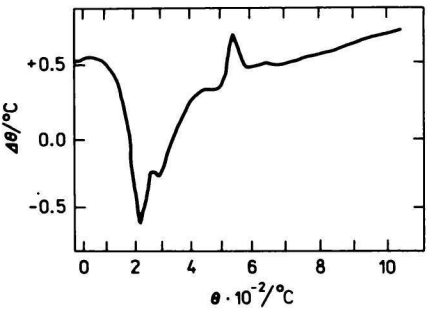

Fig. 2. DTA curve of heulandite.

Table 2

Evaluation of TGA and DTA heulandite curves

	Temperature of extrema/°C						
TGA	200	280					
DTA	220	280	380	520	600	540 exo	620 exo

determined on the basis of the DTA curve evaluation) was carried out in a quartz ampoule, which was placed in the electric resistance furnace, controlled by the pulse regulator. The ampoule was evacuated by an oil rotatory air pump and heated always for the period of 3 h to the determined temperature. The temperature was scanned by the thermocouple directly in the sample. When the decomposition was terminated and after cooling (always in the vacuum), the sample was poured on with a Nujol oil. Then the vacuum was removed and the sample was applied for other measurements.

The infrared spectra of the isothermal decomposition products were measured on the polycrystallic material on the double-beam Perkin—Elmer 325 spectrometer in the wavenumber region of 400—4000 cm^{-1} in a Nujol emulsion under the laboratory temperature and pressure. The results of the infrared measurements are shown in Fig. 3 and Table 3. The spectra were evaluated on the basis of the literature data [9, 14, 15].

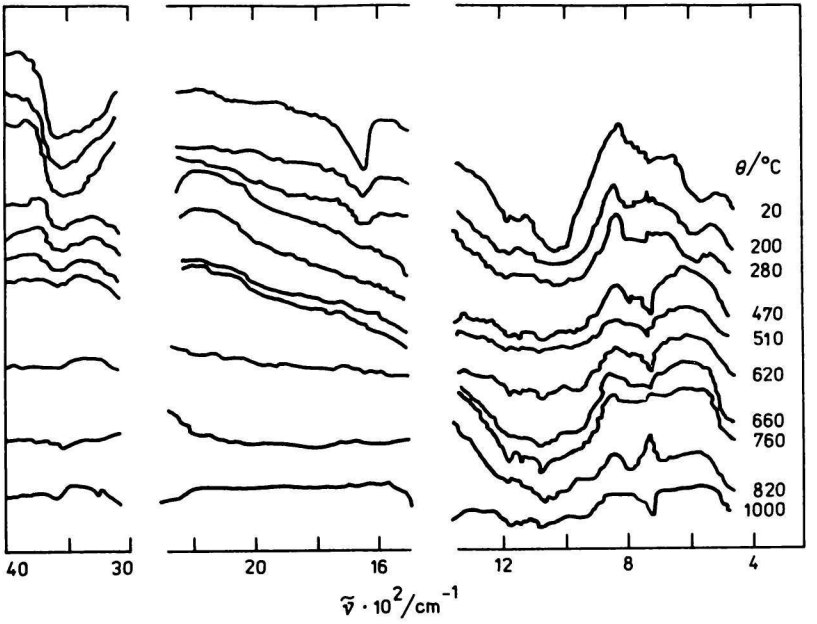

Fig. 3. Infrared absorption spectra of the isothermal decomposition products of heulandite (400—4000 cm^{-1}); Perkin—Elmer 325, Nujol oil.

Table 3

Infrared absorption spectra of the isothermal decomposition products of heulandite

θ/°C	Vibration							
	O—H stretch.	H_2O bend.	T—O stretch.	T—O stretch.	T—O stretch.	H_2O libr.	T—O bend.	Complex Al
	$\tilde{\nu}$/cm^{-1}							
20	3360—3620 vs	1620 vs	1190 w	990—1080 vs	760 w	590 m	440 m	—
200	3430—3620 vs	1610 s	1200 w	950—1110 m	790 m	610 m	440 m	—
280	3420—3620 vs	1605 m	1180 vw	950—1110 m	750—790 m	590 m	440 s	—
470	3500—3610 m	1600 infl	1160 vw	980 w	740 m	—	440 s	1140 m
		—	1180 vw	1090 w				
510	3500—3610 m	—	1160 vw	980 w	760 m	—	450 s	1140 m
			1180 vw	1090 w				
620	3500—3590 m	—	1150 vw	980 w	750 m	—	450 s	1140 m
			1180 vw	1090 m				
660	3550 w	—	1150 vw	960 w	750 m	—	450 vw	1140 vw
			1180 vw	1090 m				
760	3500 vw	—	1150 w	1090 m	740—790 w	—	450 vs	—
			1180 w					
820	3500 vw	—	1180 w	1090 m	795 m	—	450 vs	—
1000	3550 infl	—	1160 vw	1090 m	750 m	—	460 m	—
			1180 w					

vs — very strong, s — strong, m — medium, w — weak, vw — very weak; T = Si, Al.

The diffraction measurement of the X-ray radiation on the polycrystallic samples of the decomposition products was performed by means of the Guinier chamber ENRAF-NONIUS under vacuum (water pump) and laboratory temperature. For the diffraction the CuK_α radiation ($\lambda = 0.15418$ nm) and the internal synthetic standard α-Al_2O_3 were used. The X-ray diffraction records on the film material were evaluated on the densitometer Joyce—Loebel III and the subtracted angles 2Θ inversed on the values of the interplanar distances $d(hkl)$. After the indexing conformably to the calculated diffraction patterns [16], the data, thus prepared, were used for the calculation [17] of the more precise lattice parameters (Table 4).

Table 4

Shift of the lattice parameters of heulandite with increasing temperature

θ/°C	Lattice parameters 10^4/nm		
	{a}	{b}	{c}
20	17610 (5)	17821 (5)	7370 (3)
200	16021 (5)	17902 (5)	7851 (5)
280	12314 (10)	18011 (10)	10241 (10)
470	8645 (10)	18124 (10)	14152 (10)

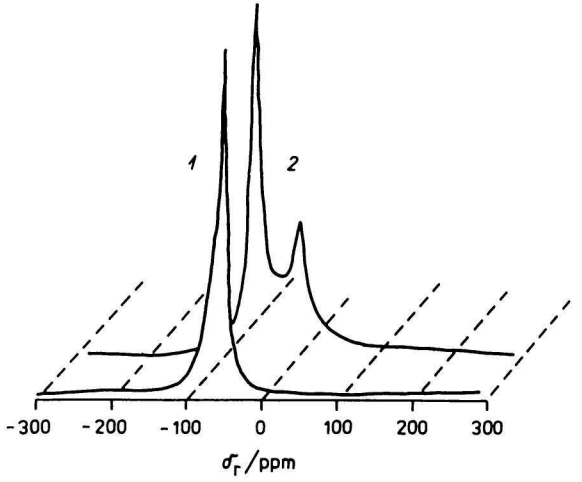

Fig. 4. NMR spectrum of ^{27}Al heulandite.
Bruker CXP-360; 93.8 MHz, pulses 3 μs; magic angle spinning 4.3 kHz.
1. Spectrum of the original sample; *2.* spectrum after the dehydration of the sample at 470 °C.

The NMR spectra of ^{27}Al were measured on the polycrystallic samples of the original heulandite and after the dehydration at 470 °C on the spectrometer Bruker CXP-360 at 93.8 MHz, pulse time 3 μs (1 with repeating), magic angle spinning 4.3 kHz. The spectra record is shown in Fig. 4 [18].

Discussion

As it is shown by the TGA curve (Fig. 1), the dehydration of heulandite is realized in two steps with the greatest speed of losing the mass at the temperature of 200 °C and 280 °C. Heulandite loses at this process 14.4 % of its mass, *i.e.* in the first step 6.5 % and in the second one 7.9 %. According to the results of chemical analysis, heulandite contains 15.72 % of water. That means that after the dehydration 1.32 % of H_2O remains in the heulandite structure.

From the structural measurements [19, 20] it can be judged that the two steps correspond to two types of water, bound with variously long coordination bonds with the adjacent atoms (I. H_2O bond from 0.259 to 0.267 nm; II. H_2O bond from 0.211 to 0.251 nm). That means that in the first step the more freely bound water molecules are dehydrated and in the second one those bound with a greater strength.

The DTA curve (Fig. 2) confirms these measurements. The great endothermic tolerance at 220 °C and the lower one at 280 °C correspond to two steps of dehydration, the other endothermic tolerances to the terminating dehydration, and the exothermic tolerances correspond to the structural changes of heulandite. The course of these effects (excluding the shift of temperatures) is in principle conformable with that described in the previous papers [8, 9, 11].

In the infrared spectra of the isothermal decomposition in the range of all studied temperatures (Fig. 3) we can follow the stretching vibrations of hydroxyl groups in the wavenumber region of 3360—3620 cm^{-1} [9], while the bending vibrations of H_2O at the wavenumbers of 1600—1620 cm^{-1} can be observed only up to the temperature of 280 °C. That means that in the course of dehydration the remaining water is split in a heterolytic way by the effect of cations and the arisen free protons attack the bridge oxygens in the bridge Al—$\overset{(-)}{O}$—Si under the formation of the hydroxyl structural groups, which remain up to 1000 °C. The torsion vibration of H_2O at the wavenumbers of 590—610 cm^{-1} can be also found up to the temperature of 280 °C [15]. Within the range of all temperatures there can be seen in the infrared spectra the stretching vibrations of the bonds (Si, Al)—O in the wavenumber range 950—1110 cm^{-1} and 745—795 cm^{-1} [14]. That means that the tetrahedral linkage arrangement in tetrahedrons $(Si, Al)O_4$ remains up to the temperature of 1000 °C. Also the bending vibrations of the tetrahedral linkage being within the wavenumber region of 440—460 cm^{-1} can be found in the whole range of the studied temperatures up to 1000 °C. The external vibration between

the tetrahedrons being in the wavenumber region of 1150—1200 cm^{-1}, can be found in the spectra of all decomposition products. It results from this fact that in the course of formation of the new phases the arrangement on the short distance of certain structure fragments remains preserved. From the temperature of 470 °C at $\tilde{\nu} = 1140\ cm^{-1}$ a relatively strong band of the stretching complex vibration $Al^{3+}(OH^-...H^+)$ begins to appear. That testifies that in the course of the thermal treatment a certain part of the Al atoms passes into the cation positions and forms a complicated aquacomplex of the type $Al^{3+}(OH^-...H^+)...Ca^{2+}$ [21]. This one can arise only by such a mechanism that in the course of the temperature increase the heavy polarized cation Ca^{2+} affects the bridge Al—O—Si in tetrahedron and

successively occurs the separation of complex and the destruction of the tetrahedral linkage.

The formation of a complex at the temperature of 470 °C was also proved by the NMR spectra of ^{27}Al, when besides the maximum with a chemical shift + 59 ppm belonging to $Al(OSi)_4$ unit [18] arises the satelite maximum with a shift of + 19 ppm, which can be assigned to the complex $Al^{3+}(OH^-...H^+)$ [18].

When studying the diffractograms of the decomposition products under the increasing temperature we can observe up to the temperature of 280 °C the size decrease of the interplanar distances *d* at the reflexes *hkl* 020, 001, 220, 310, 401, 421, 002, 510, 042, 623, 082, and 840 of heulandite, while from the temperature of 470 °C upwards there can be found in the diffractograms the reflexes of high values *d* (002, 510, 530, 261, 223) which are enlarging conformably to the increasing temperature and at the temperatures exceeding 620 °C there already appear the reflexes of anorthite, wairakite, and SiO_2, which are overlapping in some cases. Thus it can be resulted that at the dehydration the modification B is formed, while from the temperature of 470 °C upwards the crystal lattice is destroyed and the amorphous phase is formed besides the fragments of the heulandite structure. From this phase, at the temperature exceeding 620 °C a mixture of wairakite, anorthite, and α-SiO_2 arises. The formation of the minerals is terminated at about 1000 °C.

As seen from Table 4, the parameters *b* and *c* of the basic crystal cell increase with the increasing temperature, while the parameter *a* is reduced up to the temperature of 470 °C. At higher temperatures the lattice parameters could not be precisely determined from the experimental data.

Conclusion

When studying the thermal stability of heulandite it can be found that its crystal structure is stable up to the temperature of 280 °C. At higher temperatures the

metastable phase B with $3H_2O$ and lattice parameters $a = 0.8645$ nm, $b =$ $= 1.8126$ nm, $c = 1.4152$ nm begins to be formed. Regarding the study of the diffraction patterns the pseudoorthorhombic symmetry of this phase can be expected. This phase decomposes at the temperatures exceeding 470 °C into the phase with the preserved skeleton fragments $[(Si, Al)O_4]_n$ arranged on the short distance.

Above the temperature of 620 °C, the mixture of wairakite, anorthite, and SiO_2 begins to appear from this phase. In the process of dehydration the hydroxyl groups are formed, which are bound in the structure of the complicated complex till the high temperatures.

References

1. Barrer, R. M. and Langley, D. A., *J. Chem. Soc. 1958*, 3804.
2. Barrer, R. M. and Langley, D. A., *J. Chem. Soc. 1958*, 3811.
3. Barrer, R. M. and Langley, D. A., *J. Chem. Soc. 1958*, 3817.
4. Smith, J. V., *J. Chem. Soc. 1964*, 3759.
5. Mumpton, F. A., *Amer. Mineral. 45*, 351 (1960).
6. Barrer, R. M., *Proc. Roy. Soc. A167*, 393 (1938).
7. Koizumi, M. and Kiriyama, R., *Mineral. J. 1*, 36 (1953).
8. Peng, C. J., *Amer. Mineral. 40*, 834 (1955).
9. Breck, D. W., *Zeolite Molecular Sieves. Structure, Chemistry and Use.* Wiley, New York, 1974.
10. Barrer, R. M. and Bratt, G. C., *J. Phys. Chem. Solids 12*, 130 (1959).
11. Mumpton, F. A., *Amer. Mineral. 45*, 351 (1960).
12. Barrer, R. M. and Vanghan, D. E. W., *Surface Sci. 14*, 77 (1969).
13. Breger, I. A., Chandler, J. C., and Zubovic, P., *Amer. Mineral. 55*, 825 (1970).
14. Flaningen, E. M., Khatami, H., and Szymanski, H. A., *Advan. Chem. Ser. 101*, 201 (1978).
15. Milkey, R. G., *Amer. Mineral. 45*, 990 (1960).
16. Weiss, Z. and Krajíček, P., unpublished results.
17. Buruham, C. W., *Washington Year Book 61*, 132 (1962).
18. Lippmaa, E., Mäggi, M., Samoson, A., Engelhardt, G., and Grimmer, A. R., *J. Amer. Chem. Soc. 102*, 4889 (1980).
19. Merkle, A. B. and Slanghter, M., *Amer. Mineral. 52*, 273 (1967).
20. Merkle, A. B. and Slanghter, M., *Amer. Mineral. 53*, 1120 (1968).
21. Ross, S. D., *Inorganic Infrared and Raman Spectra.* McGraw-Hill, London, 1972.

Translated by F. Pechar